CrossMark

ORIGINAL PAPER

Aboveground biomass of naturally regenerated and replanted semi-tropical shrublands derived from aerial imagery

Arjun Adhikari[1,4] · Jian Yao[2] · Mitch Sternberg[3] · Kelly McDowell[3] ·
Joseph D. White[1,2]

Abstract Rapid assessment of plant size and population densities is important for estimating biomass over large areas, but it has often been limited by methods requiring intensive labor and resources. In this study, we demonstrate how shrub biomass can be estimated from fine-grained aerial photographs for a large area (23,000 ha) located in the Lower Rio Grande Valley, Texas, USA. Over the past 30 years, refuge land management has included the replanting of native shrubs to promote the restoration of wildlife habitat and carbon sequestration. To assess shrub regrowth, we developed a method to estimate individual shrub canopy areas from digital aerial imagery that was used to calculate biomass from allometric equations. The accuracy of the automated delineation of individual canopies was 79 % when compared to that of hand-digitized shrub canopies. When applied to photographs across the refuge, we found higher shrub densities for older naturally regenerated sites (174 individuals ha^{-1}) compared to those of younger replanted sites (156 individuals ha^{-1}). In contrast, naturally regenerated sites had less biomass (3.43 Mg ha^{-1}) than replanted sites (4.78 Mg ha^{-1}) indicating that shrubland restored for habitat conservation has

the potential to sequester more carbon in a shorter period. There was an inverse relationship between aridity and aboveground shrub biomass for replanted sites in the drier west ($p < 0.05$). We found a difference in predicted biomass among shrub species in replanted sites that was also associated with climate ($p < 0.05$). We conclude that the canopy of individual shrubs detected from remote sensing can be used to estimate and monitor vegetation biomass over large areas across environmental gradients.

Keywords Remote sensing · Allometric equations · Soil-adjusted vegetation index · Carbon storage

Introduction

The importance of ecosystems dominated by shrub vegetation is often neglected because they are considered as successional transient communities (Thompson and DeGraaf 2001), dominated by nuisance species (Van Auken 2000), which are difficult to manage (Schlossberg et al. 2010). Shrubland ecosystems have the potential to store a large amount of carbon in the soil and in plant tissues; the latter can be enhanced with proper management of shrublands (Wenhiu et al. 2014; Adhikari and White 2016). It is important to quantify shrub biomass because decomposition-resistant woody tissue reduces the ratio of vegetation to soil carbon fluxes over long time scales (Lioubimtseva and Adams 2004; Litton and Kauffman 2008; Burquez et al. 2010).

Field-based measurements of shrub cover, density, and woody biomass require considerable time and resources (Koch et al. 2006). Fine-grained remote sensing data can complement intensive field monitoring where plant density, canopy, and biomass changes have been evaluated

✉ Arjun Adhikari
arjun.adhikari@montana.edu

1   Department of Biology, Baylor University, One Bear Place #97388, Waco, TX 76798, USA

2   The Institute of Ecological, Earth, and Environmental Sciences, Baylor University, One Bear Place #97205, Waco, TX 76798, USA

3   South Texas Refuge Complex, US Fish and Wildlife Service, 3325 Green Jay Road, Alamo, TX 78516, USA

4   Present Address: Department of Ecology, Montana State University, Bozeman, MT 59715, USA

consistently across a large geographic extent over time (Pollock 1994; Gougeon 1995; Culvenor 2002; Clark et al. 2004; Wang et al. 2004; Erickson and Olofsson 2005; Suganuma et al. 2006; Anaya et al. 2009). For large areas, remote sensing data have been used to quantify density and biomass of shrubs important for assessing carbon sequestration potential (Asner et al. 2009). Primarily, remote sensing data can detect individual plant crowns that correspond with aboveground biomass (White 2001; Wang et al. 2004; Suganuma et al. 2006; Anaya et al. 2009; Katoh et al. 2009).

Various methods have been developed to identify individual plants from remote sensing data. Pollock (1994) and Larsen and Rudemo (1998) developed a template matching method generating different synthetic tree crown models with different illumination, viewing angle, and sizes of different tree species. The valley following method developed by Gougeon (1995) defined plant crown borders based on the detection of local digital number (DN) minima within a specified search radius. Wulder et al. (2000) used local maxima filtering with fixed or variable window sizes to improve plant canopy discrimination in forested areas. The tree identification and delineation algorithm (Culvenor 2002) was developed using both local maxima and minima in a data set derived from digital multispectral video. A classification method based on image segmentation and object-oriented images was developed by Laliberte et al. (2004) to assess the shrub encroachment into New Mexico grassland. However, object-based image analyses are generally favorable for change detection but suffer from overgeneralizing canopy size and limited detection of plants with small canopy area (Stow et al. 2008). These methods have generally been based on the spectral reflectance of a plant canopy without considering the combined reflectance from the soil and canopy. Reflections from sparse and isolated canopies in shrublands are affected by high soil reflectance. This reduces the effectiveness of remote sensing in delineating individual plant canopies and highlights the need to develop a method to compensate for soil exposure.

Aboveground biomass of a single plant can be estimated by using crown areas (A_C) of shrubs where allometric equations are available (Hughes et al. 1987; Navar et al. 2002; Northup et al. 2005). Canopy area attributes, such as projected horizontal canopy shape (i.e., circular, ellipsoid), can be incorporated into locally derived, site-specific allometric equations to estimate the biomass of single plants (Hughes et al. 1987; Navar et al. 2004; Navar 2011; Northup et al. 2005; White 2001; Yao et al. 2012). Canopy areas detected by remote sensing coupled with biomass allometric equations can be used to estimate regional biomass across environmental gradients by adding up biomass from single plant crowns over mapped areas.

For this study, we first developed a shrub identification algorithm that we applied to digital aerial imagery to identify single shrub crowns while minimizing the influence of the soil background. We then estimated shrub density from the algorithm developed for shrub crown delineation. Shrub biomass was estimated using allometric equations developed for different species using remote sensing-derived crown dimensions. Derived density and biomass were then compared for naturally regenerated and replanted sites across an environmental gradient. We then assessed the outcome of the replanting of shrubs as part of the land management actions designed to enhance the sequestration of carbon and restore shrub communities.

Materials and methods

Study site

The Lower Rio Grande Valley National Wildlife Refuge (LRGVNWR) is located in the Lower Rio Grande Valley of south Texas and has been managed by the US Fish and Wildlife Service (USFWS) since its establishment in 1979. The LRGVNWR is located along the southern border of the USA with Mexico and encompasses approximately 200 km of the broad deltaic floodplain of the Rio Grande inland from the Gulf of Mexico. This area forms the northern edge of the Tamaulipan Biotic Province (Blair 1950; Fig. 1). Since 1982, about 5560 of 23,000 ha of the LRGVNWR has been replanted with native woody shrub species to re-establish native forest and shrub communities, as over 90 % of the native vegetation had been altered due to agricultural and urban development (Jahrsdoerfer and Leslie 1988; Tremblay et al. 2005). Non-native grass species and native thorny, woody shrubs dominate patches of abandoned land within a matrix of agricultural land. Shrublands within the study area are managed as important habitat for endangered feline species such as the ocelot (*Leopardus pardalis*) and jaguarundi (*Puma jaguarundis*), which utilize the dense shrubs as hiding cover (US Fish and Wildlife Service 2013, 2016). In addition to habitat, these shrublands are potentially important as terrestrial carbon sinks (Navar-Chaidez 2008).

The vegetation canopy cover of the LRGVNWR generally decreases westward from the coast of the Gulf of Mexico in south Texas as a result of low precipitation and high potential evapotranspiration (Jahrsdoerfer and Leslie 1988). The climate is semi-arid and sub-tropical with long, hot summers and short, mild winters with temperature gradients from east to west (Eddy and Judd 2003; Table 1) with 330 mean frost free days per year. The LRGVNWR has an annual average rainfall of 680 mm, potential evapotranspiration of 2200 mm, and an average mid-
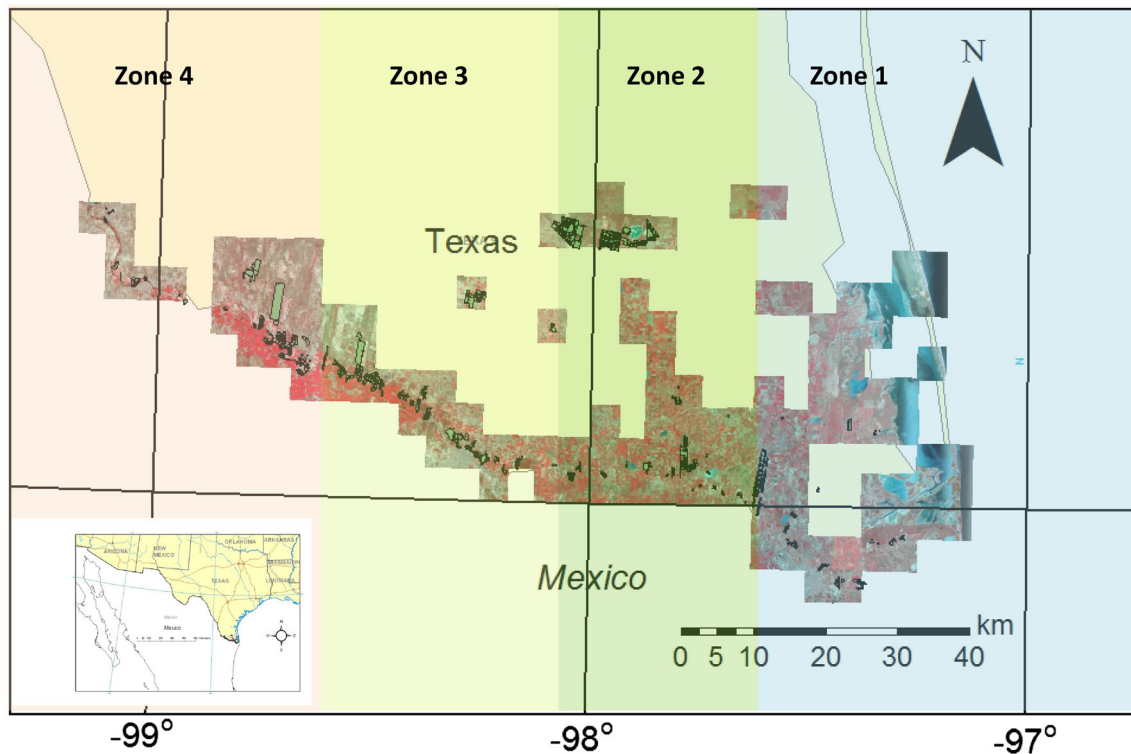
Fig. 1 The 23,000-ha Lower Rio Grande Valley (LRGV) National Wildlife Refuge follows the Rio Grande and is located along the border of the USA and Mexico. The *raster patches* inside the larger map were produced by mosaicking 170 digital orthophoto quarter quadrangles to encompass the entire LRGV. Total numbers of tracts are shown over mosaic raster. Each defined climatic zone is indicated by a *different shade of color*

Table 1 East–west climatic zone of the Lower Rio Grande Valley and 30-year mean temperature, precipitation, and potential evapotranspiration values (*PET*) of each zone Source: PRISM climate group, Oregon State University, 2013

Zone	Longitude	Mean temperature (°C)	Mean precipitation (cm)	PET (cm)	Number of tracts of naturally regenerated land	Number of tracts of replanted land
1	−97.49° to −97.10°	16.09	70.20	36.30	10	10
2	−97.89° to −97.50°	15.90	65.50	51.60	7	10
3	−98.39° to −97.9°	15.42	53.70	51.90	9	10
4	−99. 80° to −8.40°	15.00	51.40	52.50	9	10

summer vapor pressure deficit of 3.05 kPa (Rodriguez et al. 2004). Dominant spiny shrubs and trees of LRGVNWR include: *Vachellia rigidula* (Benth.) Seigler & Ebinger, *Sideroxylon celastrinum* (Kunth) T.D. Penn, *Celtis ehrenbergiana* (Klotzsch) Liebm., *Condalia hookeri* M.C. Johnst., *Diospyros texana* Scheele, *Forestiera angustifolia* Torr., *Zanthoxylum fagara* (L.) Sarg., and *Prosopis glandulosa* Torr. A diversity of grasses, forbs, and succulents are also common in the valley. For this study, areas of successional shrublands with no records of replanting treatments were considered and are referred to as "naturally regenerated sites." We assumed that natural regeneration of shrubs has occurred through reseeding by remnant shrubs within the landscape and from the existing, local soil seed bank. Land tracts with active replantation after the 1980s are considered and referred to as "replanted sites." Tracts in this study refer to individual properties purchased and managed by the USFWS. However, the federal acquisition of abandoned agricultural lands for the refuge began in 1979; therefore natural and replanted sites are considered comparable.

Data preparation

In the study area, aerial color infrared imagery in the form of digital orthophoto quarter quadrangle (DOQQ) data, were acquired from the Texas Natural Resources Information System (TNRIS; www.tnris.state.tx.us). These data

have 0.5-m spatial resolution with three spectral bands in the green (495–570 nm), red (R; 620–750 nm), and near-infrared (NIR; 750–950 nm) wavelengths. For our analysis, we obtained 170 individual quarter quadrangles. The majority of the DOQQ data were acquired from April to September 2008, during which woody shrubs maintained crown foliage. These images showed higher bare soil exposure indicating senescent understory herbaceous vegetation likely associated with shading and water competition from the shrub overstory (Peltzer and Köchy 2001). Complete coverage of the LRGVNWR was accomplished by using data from January to March 2009. For the analysis presented in this study, we analyzed 75 tracts chosen randomly representing a total of 835 ha. A database on replantation developed by the USFWS was used to help randomly select replanted tracts as part of the total of 75 tracts. Our analysis is based on 35 tracts assigned as naturally regenerated and 40 tracts assigned as replanted sites.

Radiometric normalization

The DOQQ images obtained from TNRIS were originally radiometrically balanced between the quadrangles using Inpho's OrthoVista 4.0 (Trimble Navigation, CA; TNRIS 2009). However, in our initial analysis, we found that DNs of coincident pixels in overlapping areas of adjacent DOQQs had different values. These differences were likely due to skewed distributions of DN values for each image associated with varying land cover present in each individual quadrangle. To minimize differences in DN values between quadrangles, we performed histogram matching (HM) on each quadrangle using a reference DOQQ dataset. In this procedure, histograms of the working image were adjusted to be as close as possible to the mean and SD of a reference image (Helmer and Ruefenacht 2005; Mitchell 2010; Richards and Xiuping 1993; Yang and Lo 2000). Because of the need for radiometric consistency among all our data, we used a single DOQQ dataset chosen arbitrarily as the reference image for HM of all other DOQQ data.

Crown delineation algorithm

To delineate shrub crowns from the DOQQ data, we developed a novel algorithm that first reduced the soil's influence (Fig. 2). After applying the HM to DOQQ data, we calculated the soil-adjusted vegetation index (SAVI) (Gilabert et al. 2002; Huete 1988) using R and NIR wavelengths (Eq. 1).

$$\text{SAVI} = (\text{NIR} - \text{R})(1 + L)/(\text{NIR} + \text{R} + L) \qquad (1)$$

where L is a soil-brightness-dependent correction factor. Gilabert et al. (2002) suggested a value of 0.5 for L for

Fig. 2 **a** Flow chart of algorithm development for delineation of individual shrub crowns from the digital orthophoto quarter quadrangle (*DOQQ*) images, **b** stacks of images show a subset of the DOQQ data on a tract of Lower Rio Grande Valley National Wildlife Refuge used to initially test our canopy crown delineation algorithms. The site was replanted with native shrubs during the 1990s. The *white dots* represent individual shrub crowns, and shrub polygons after converting the images into vectors. *Each polygon* represents a single shrub
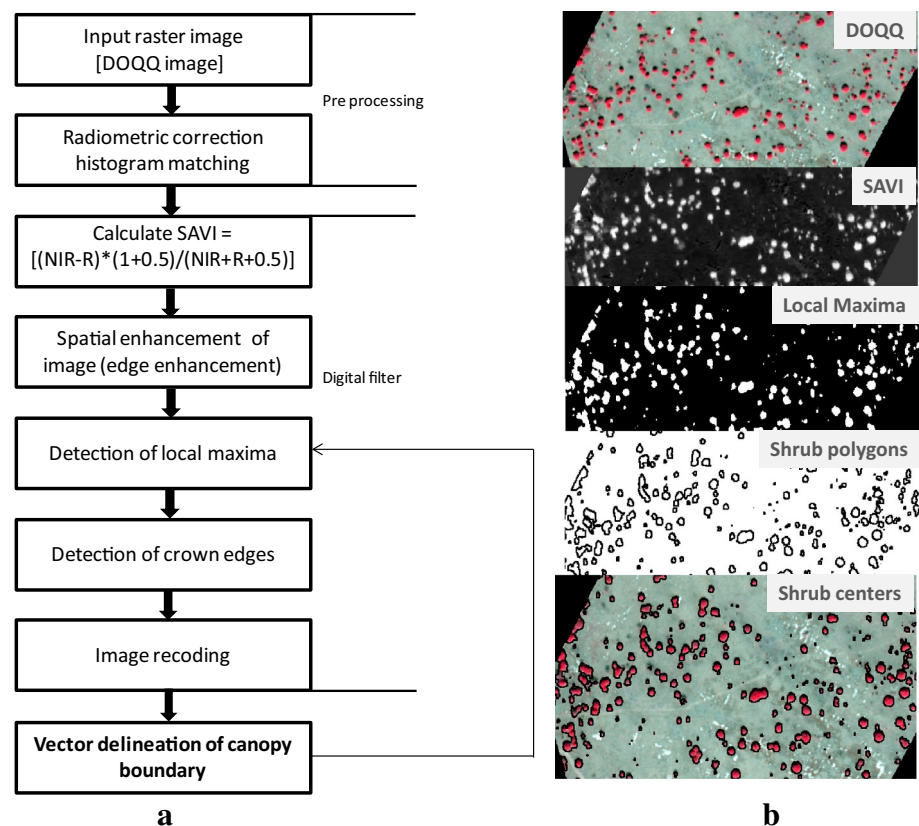
-1	-1	-1
-1	17	-1
-1	-1	-1

a

1	-1	-1
-1	9	-1
-1	-1	-1

b

Fig. 3 Matrices for a 3 × 3 convolution kernel filter for **a** edge enhancement of image, and **b** local maxima determination of image. Both kernels were used to enhance the image during image processing for shrub density and biomass estimation

areas with sparse vegetation canopies, which we used in our calculation.

Next, a 3 × 3 convolution filter was applied to potentially enhance the radiometric edges of adjoining shrub canopies (Fig. 3a). This was followed by application of another 3 × 3 convolution kernel filter to detect local maxima in the SAVI data (Fig. 3b). The maximum value was then used as the new center pixel value where a larger value was identified among the eight surrounding pixels. Initially, pixels dominated by shrubs were discriminated from those with soil and herbaceous vegetation using a threshold SAVI value. This threshold value was determined iteratively using the image produced following calculation of the local maxima. To determine this threshold value, a reference dataset was created from a subset of the DOQQ image for a test site (22 ha) within the LRGVNWR that was replanted with native shrubs during the 1990s. A replanted site was chosen because the regular spacing of the shrubs associated with replantation allowed for easy visual identification of individual shrub crowns. For 563 individual shrub crowns, a polygon was hand-digitized from the displayed subset DOQQ image.

Our initial threshold value was set arbitrarily to a value of 0.05, with pixel SAVI values greater than or equal to this value categorized as a shrub crown. The boundary between shrub and non-shrub pixels was then determined using a search function around shrub pixels. Contiguous shrub pixels were assumed to represent a single shrub crown and the raster boundary determined from the search analysis was converted from the raster format to vector. Each crown encompassed by a closed vector polygon was considered as a single shrub. The ratio of the number of the automated detected shrubs to hand-digitized crowns was then calculated and expressed as a percentage. The threshold value was calibrated by changing the initial value of 0.05 and the percentage ratio of automated to hand digitized number of crowns recalculated. The final SAVI threshold value that produced the closest number of shrubs with a ratio <1.0 was then used for processing all subsequent data (Table 2).

For each delineated shrub, a vector polygon was derived from the raster data with the long and short axes of each elliptical crown polygon calculated using Python software

Table 2 Different soil-adjusted vegetation index (*SAVI*) values used to calibrate a threshold value from a SAVI image of the test site (22 ha) are shown. A threshold SAVI value of 0.2 was found to identify the number of shrubs closest to the hand-digitized shrub number for the test area without exceeding 100 %

Different SAVI values used for shrub estimation	Number of shrub individuals identified by new algorithm	% Shrub individuals identified by new algorithm
0.05	778	138
0.10	637	113
0.15	581	103
0.20	537	95
0.25	506	89
0.30	491	87
0.35	482	85
0.40	441	78
0.45	425	75
0.50	403	71
0.55	392	69
0.60	372	66

(Patterson 2011). These axes values for each shrub were used to calculate A_C of each shrub (Eq. 2). Calculation of these axes replicated the field measurements by Northup et al. (2005) that we later used to estimate aboveground biomass based on their allometric equations

$$A_C = [(\text{long axis}/2) \times (\text{short axis}/2) \times \pi] \qquad (2)$$

For areas with densely growing shrubs, we had difficulty delineating individual shrub crowns. To minimize this error, we divided any A_C by a derived area >12 m² by 12.0, assuming that the crown was anonymously large. This assumption was based on an average A_C value of 12 m² with a mean height of 5.1 m estimated using 50 randomly selected shrubs from an undisturbed site within LRGVNWR (26.19°N, −98.07°W).

Error assessment

We confirmed shrub density estimation by visually identifying individual shrubs that were counted from 20 randomly selected sites with mean tract areas of 9.16 and 7.63 ha for naturally regenerated and replanted sites, respectively. To assess the accuracy of estimated shrub density, we calculated the ratio of the number of shrubs identified by the remote sensing method to those visually identified per hectare expressed as a percentage.

Long and short axes of observed crowns were assessed first by hand-digitizing by drawing polygons around the crown boundaries of 450 shrubs across randomly selected naturally regenerated and replanted sites for each climatic zone. The root mean square error (RMSE) and percent bias

(PBIAS) were calculated for shrub density, long and short axis values per shrub from the data derived from remote sensing and observed values by:

$$RMSE = \sqrt{\sum_{i=1}^{n} \frac{(\hat{y}_i - y_i)^2}{n}} \qquad (3)$$

$$PBIAS = \sum_{i=1}^{n} \frac{(\hat{y}_i - y_i)^2}{n} \times 100 \qquad (4)$$

where, $\hat{y}_i$ is the remote sensing value, y_i is the hand-digitized value, and n is number of observations for both equations.

Density and biomass estimation

Biomass of each shrub was estimated from derived values of A_C based on allometric equations (in grams) developed by Northup et al. (2005) for six shrub species commonly found in the LRGVNWR (Appendix A). Six species-specific biomass values were calculated for each shrub identified in 75 randomly selected tracts for a total area of 835 ha. Because identification of shrub species was not possible from the DOQQ, we calculated the biomass of each of the six species from the allometric equations and averaged these values. Average shrub density, A_C per shrub, biomass per shrub, and biomass per hectare were calculated for each tract.

Climate zones

To assess effects of climate factors on shrub biomass and density, we partitioned the study area into four climatic zones based on approximate equal distances from east to west (Fig. 1; Table 1). To characterize the climate patterns of these zones, average temperature, precipitation, and potential evapotranspiration for each zone were calculated from meteorological data of the study area for 30 years (1981–2010) extracted from the Prism Climate Group's dataset (http://prism.oregonstate.edu/). Numbers of tracts analyzed for each zone of naturally regenerated and replanted sites are given in Table 1.

Statistical analysis

Shrub biomass, density, and A_C data were not normally distributed and could not be normalized using standard transformation techniques. Comparison of means of shrub density, A_C, biomass per plant, and biomass per hectare within and between the naturally regenerated and replanted sites, and climatic zones across the LRGVNWR, were assessed with the non-parametric Mann–Whitney test. In addition, we used the Kruskal–Wallis test to assess differences in mean shrub density, A_C, biomass per shrub, and biomass per hectare among the climate zones of naturally regenerated and replanted sites across the LRGVNWR. Since biomass estimation included samples generated from different tracts where the mean value may vary between the sample tracts, pooled variance was used to estimate the SEs of shrub density, A_C per shrub, and biomass per unit area for each climatic zone. The significance level was determined at $p = 0.05$.

Results

Remote sensing, shrub size, density, and biomass

A calibrated threshold value of 0.2 for the SAVI data was determined as the value that delineated the highest proportion (95 %) of individual shrubs, with 537 remotely detected individuals identified out of 563 shrubs visually identified within the 22-ha test area (Fig. 2; Table 2). By applying this value across the study area, we estimated shrub densities of 174 and 156 shrubs ha^{-1} for naturally regenerated and replanted sites, respectively. Secondary confirmation of remotely sensed and visually identified shrub densities showed a detection accuracy of 72 % shrub individuals for naturally regenerated sites and 86 % shrub individuals for replanted sites.

The RMSE analysis of estimated shrub density was 13 shrubs ha^{-1} for naturally regenerated and 14 shrubs ha^{-1} for replanted sites. On average, the RMSE for the short and long axes of a shrub crown were 0.12 m and 0.19 m for naturally regenerated sites, respectively, and 0.18 m and 0.25 m for replanted sites, respectively. The percent bias for shrub density and shrub A_C (long and short axes) was <1 %.

Crown dimension and biomass analysis

The average A_C per shrub in naturally regenerated and replanted sites was 9.61 m^2 and 8.53 m^2, respectively. The average aboveground biomass per shrub was 15.85 kg for naturally regenerated sites compared to 16.00 kg for the replanted sites. Aboveground biomass per shrub was significantly different among the species. The predicted biomass per shrub for *D. texana* (24.48 ± 2.39 kg), *C. hookeri* (22.04 ± 2.21 kg), and *P. glandulosa* (17.45 ± 1.75 kg) was higher than that for *V. rigidula* (9.56 ± 0.95 kg), *C. ehrenbergiana* (12.63 ± 1.20 kg), and *Z. fagara* (9.37 ± 0.78 kg) ($p < 0.05$; Fig. 4). The estimated average biomass of naturally regenerated sites was 3.43 Mg ha^{-1} on LRGVNWR compared to 4.78 Mg ha^{-1} on its replanted sites.
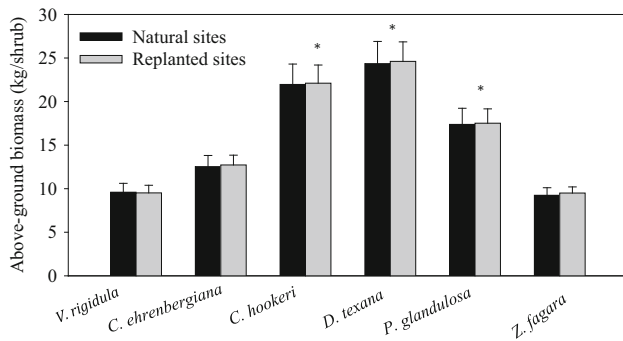
Fig. 4 Average aboveground biomass per shrub of six species with 95 % confidence intervals (CIs; *error bars*) for naturally regenerated and replanted sites. *Asterisk* denotes significantly different estimated aboveground biomass per shrub ($p < 0.05$)

Climatic zone comparison

The estimated shrub density per hectare was 176 ± 47, 160 ± 47, 226 ± 57, and 135 ± 18 for naturally regenerated sites of climatic zones 1, 2, 3, and 4 compared to 188 ± 43, 82 ± 13, 144 ± 35, and 208 ± 42 for replanted sites of the respective zones (Fig. 5). Shrub species' densities differed for the types of site among the zones. For example, replanted sites of zone 1 had higher shrub density than those of zones 2 and 3 ($p < 0.05$; Fig. 5). Shrub density also differed between naturally regenerated and replanted sites within a zone. For example, naturally regenerated sites of climate zone 2 had a significantly higher number of shrub individuals per hectare than the replanted sites ($p < 0.05$; Fig. 5).

Average A_C per shrub was 8.97 ± 0.87, 9.20 ± 1.10, 9.99 ± 0.96, and 10.28 ± 0.79 m^2 for naturally regenerated sites of climatic zones 1, 2, 3 and 4, respectively (Fig. 6). For naturally regenerated sites, zone 4 had larger A_C per shrub compared to zone 1 ($p < 0.05$; Fig. 6). A_C per shrub of replanted sites was significantly different among zones, with 9.00 ± 0.88, 7.28 ± 0.76, 9.77 ± 0.90, and 9.53 ± 0.89 m^2 for climatic zones 1, 2, 3, and 4, respectively ($p < 0.05$; Fig. 6). For replanted sites, climatic zones 3 and 4 had significantly larger A_C per shrub compared to

zone 2 ($p < 0.05$; Fig. 6). A_C also differed per shrub within a zone for two types of site. For example, naturally regenerated sites had larger A_C per shrub than replanted sites in climatic zone 2 (Fig. 6; $p < 0.05$).

The estimated aboveground biomass for climatic zones 1, 2, 3, and 4 was 15.23 ± 2.97, 19.69 ± 3.38, 11.77 ± 3.13, and 16.69 ± 3.41 kg per shrub for naturally regenerated sites and 14.65 ± 2.96, 12.74 ± 2.57, 17.33 ± 2.67, and 19.28 ± 2.59 kg per shrub for replanted sites, respectively. The species were significantly different in average aboveground biomass per shrub for different types of site. For example, *D. texana*, *C. hookeri*, and *. glandulosa* had higher biomass per shrub with values of 24.35 ± 2.55, 21.96 ± 2.35, and 17.38 ± 1.85 kg for naturally regenerated sites and 24.61 ± 2.23, 22.21 ± 2.08, and 17.52 ± 1.65 kg for replanted sites, respectively ($p < 0.05$; Fig. 5). This study also found difference in biomass per shrub among the zones for the same type of site, where replanted sites in zone 4 had higher shrub biomass per shrub compared with zone 2 ($p < 0.05$; Fig. 7).

The aboveground biomass of naturally regenerated sites was 2.58 ± 0.66, 2.31 ± 0.32, 2.39 ± 0.53, and 1.74 ± 0.24 Mg ha^{-1}, and of replanted sites 2.51 ± 0.52, 1.09 ± 0.21, 2.05 ± 0.38, and 3.63 ± 1.18 Mg ha^{-1} for climatic zones 1, 2, 3, and 4, respectively (Fig. 7). Aboveground biomass differed among the zones within a site and between the sites. For example, zone 4 had higher aboveground biomass per hectare compared to zone 2 for replanted sites ($p < 0.05$; Fig. 7). Similarly, in zone 2, naturally regenerated sites had higher aboveground biomass per hectare than replanted sites ($p < 0.05$; Fig. 7).

Discussion

Remote sensing of shrub density, crown spread, and biomass estimation

The major contribution of this study is the development of a new approach for the automatic detection of individual

Fig. 5 **a** Average shrub density, **b** average aboveground biomass (Mg/ha) in four zones of naturally regenerated and replanted sites shown with 95 % CI (*error bars*). *Asterisk* denotes significantly different shrub density and average aboveground biomass (Mg/ha) in four zones
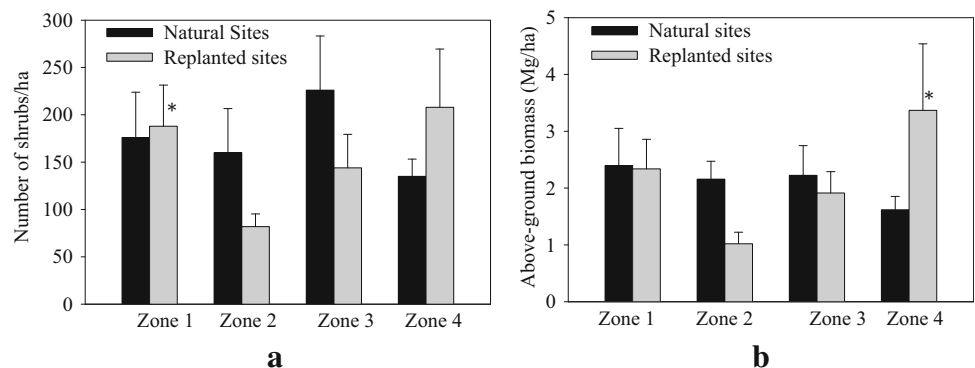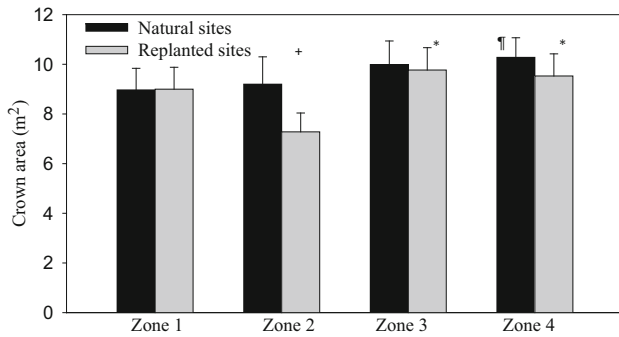
Fig. 6 Average individual shrub crown area (m^2) for naturally regenerated and replanted sites shown with 95 % CI (*error bars*). The *pilcrow*, *plus sign*, and *asterisk* denote significantly different crown areas

shrubs and their crowns from fine-resolution multispectral remote sensing data. The shrub crown dimensions can be used in shrub vegetation and biomass monitoring. This approach has important implications for land management as it allows the assessment of carbon sequestration and habitat restoration on a broader scale. However, variation in the DN between the DOQQs and the presence of soil brightness in the data were major challenges to implementing this method over a large spatial extent. Normalizing the radiometric data among quadrangles and obtaining a uniform distribution of DN values for all

analyzed imagery was key in developing a consistent database to derive a uniform threshold SAVI value.

Soil brightness in our dataset could have reduced R reflectance compared to the NIR reflectance of vegetation resulting in inaccurate detection of vegetation in the image (Colwell 1974, Major et al. 1990). Using SAVI enhances the contrast between the soil and vegetation by lowering soil background-induced variation and increase the discrimination of shrubs from remote sensing data (Huete 1988; Qi et al. 1994; Lyon et al. 1998). The threshold SAVI value of 0.20 was found to be effective for the maximum separation of woody shrub crowns from the surrounding soil background. While the DOQQ obtained in 2009 showed a higher apparent live foliage shrub and herbaceous ground vegetation with minimal soil exposure compared to those of 2008, distinguishing shrubs from the calibrated threshold SAVI value generated a consistent shrub detection across all tracts. However, the algorithm tended to underestimate individual shrubs per hectare and A_C per shrub across the study sites. For some tracts, crowns forming dense homogeneous canopy could not be separated completely as many interlocking crowns were detected as single crowns (Blanco and Navarro 2003; Koch et al. 2006). Therefore, automatic delineation of single crowns can produce better results for sparse shrubland vegetation. Errors in shrub detection across the large area in this study

Fig. 7a, b Average aboveground biomass of six species in four climatic zones shown with 95 % CI (*error bars*). **a** Naturally regenerated sites, **b** replanted sites. *Asterisk* denotes significantly different aboveground biomass
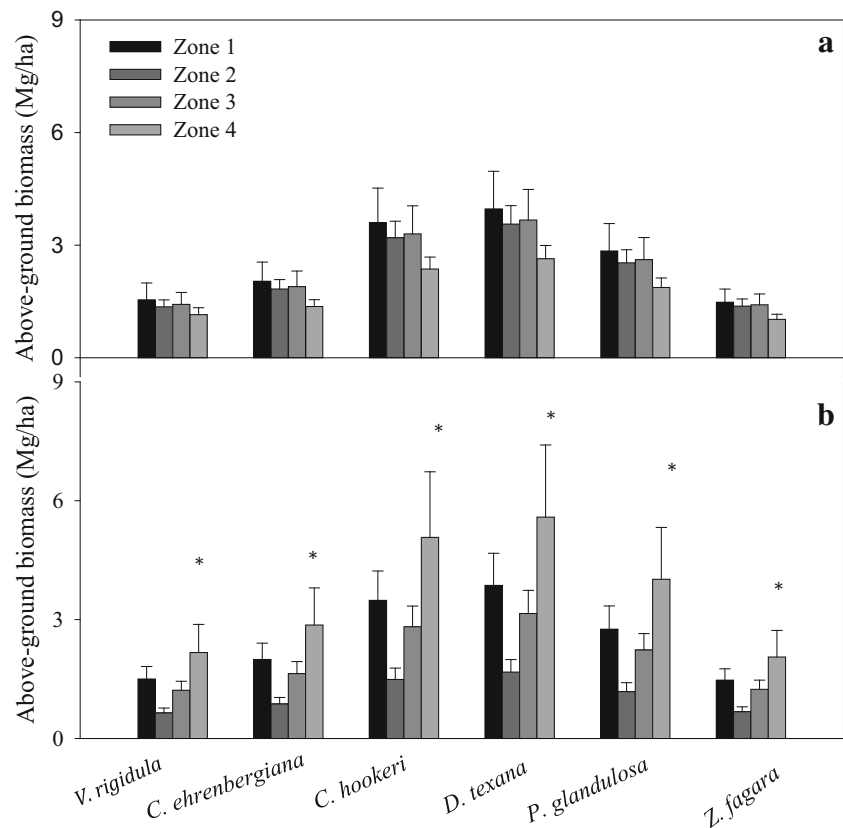
indicate that remaining variation should be considered as part of the global error in using this type of analysis for landscape assessment of shrub biomass.

Plant biomass estimated from allometric equations using remote sensing-derived crown dimensions has a considerable advantage over plot sampling for spatially extensive areas, and has the potential to capture entire plant populations. However, allometric equations for the shrub species native to these areas showed large variation in predicted biomass. Stand structure, allometry of biomass partitioning and allocation can be influenced by variations in climate, environment, and competition for resources among the species (Archer 1989; Northup et al. 2005). For example, predominately single- or few-stemmed species such as *C. hookeri*, *D. texana*, and *P. glandulosa* had higher biomass allocation to canopy components than multi-stemmed species such as *V. rigidula*, *C. ehrenbergiana*, and *Z. fagara* when estimated by basal area. The large range in biomass for the same A_C values based on the species-specific allometry indicates that the selection of species for replanting treatments influences carbon sequestration. In addition, estimation of biomass values by averaging allometric equations can be a source of error in biomass estimation at a larger scale (Kettrings et al. 2001). Despite these sources of error and environmental variation, the average biomass of 14.80 kg per shrub estimated for LRGVNWR was close to that of 13.6 kg per shrub reported by Navar et al. (2004). On an area basis, we found that the average biomass derived in this study (4.26 Mg ha^{-1}) was less than that of Navar et al. (2002) for Tamaulipan thorn shrubs of Northern Mexico (60 Mg ha^{-1}). However, this difference can be attributed to a lower shrub density of 165 shrubs ha^{-1} (data not shown) on LRGVNWR compared to 5000 shrubs ha^{-1} reported by Navar et al. (2002). This result is likely associated with land use history and site moisture. Sites sampled by Navar et al. (2002) received an annual precipitation of 1000 mm compared to that of 680 mm on LRGVNWR (Adhikari and White 2016).

Analysis of naturally regenerated and replanted sites

Multiple factors affect the relationship between stand density and biomass. During stand development, depending on initial seedling density, resource competition intensifies asymmetrically for individual plants (Holdway et al. 2008; Luyssaert et al. 2008). Ideally, in both even- and uneven-aged naturally regenerated stands, individuals compete for resources (e.g., light, water, and nutrients) where crowding may influence mortality, reduce plant density, and maximize the size of individual plants following self-thinning (Li et al. 2000). However, we did not find an influence of density on individual biomass production in naturally

regenerated sites. Differences in shrub biomass across replanted sites may be due to the effects of site-specific land use history in which intensive crop farming has resulted in reduced soil fertility of the area before establishment of the refuge (Adhikari and White 2016). Higher biomass per shrub in replanted sites compared to naturally regenerated sites was likely due to reduced competition that also limits maximum individual stand volume (Li et al. 2000; Luyssaert et al. 2008). Overall, we estimated that the total biomass fraction in replanted sites (24 % of total above-ground biomass stored) was almost equal to its area fraction (26 % of total area). This indicates that direct and indirect methods of promoting shrub establishment significantly contribute to carbon sequestration.

Environmental gradients

Limited soil water availability constrains shrub growth and survival (Montagu and Woo 1999; Rodriguez et al. 2004; Adhikari and White 2014) and determines the relationship between shrub density and biomass (Lambers et al. 1997). The Lower Rio Grande Valley is characterized by increasing aridity westwards. Inland from the Gulf of Mexico, the temperature increases and precipitation decreases, with substantial influences on the growth and survival of shrub species (Adhikari and White 2016). Therefore, we expected higher shrub density, higher biomass per shrub, larger shrub A_C, and higher biomass per hectare in the eastern part of the LRGVNWR due to this environmental setting. However, past intensive agricultural activities that may have reduced soil fertility may explain lower shrub density, lower biomass per unit area, and smaller A_C per shrub in naturally regenerated sites of zone 2 compared to replanted sites in zone 1. Zeidler et al. (2002) reported slow growth rates of plant and low biomass accumulation under similar environmental conditions in degraded arid and semi-arid land of Africa. Also, a similar explanation can be given for the higher biomass per shrub, larger A_C per shrub, and higher biomass per hectare of replanted sites in zone 4 compared to zone 2. However, naturally regenerated sites in zone 4 showed larger A_C per plant compared to those in zone 1. This is due to the aridity in zone 4, where specific plant species are better adapted with a higher growth rate, likely associated with low levels of competition (Adhikari and White 2014).

LRGVNWR shrubland, wildlife habitat and carbon sequestration

Remote sensing provides a wall-to-wall mapping capability that can help land managers devise effective methods to invest resource management capital. We have shown that remote sensing can be used to accurately assess plant

density and biomass over a large area of a conservation landscape. The application of fine-scale remote sensing data to identify individual plants and measure their crown dimensions can be very effective for sparsely distributed woody plants; such methods are important for the monitoring and assessment of types of land management. Shrubland ecosystems are important for their potential role in global carbon dynamics, as they comprise 30 % of terrestrial carbon stored in live biomass and soil (Bechtold and Inouye 2007; Lal 2004; Piao et al. 2009). This study showed that the carbon sequestration capacity of shrubland ecosystems could be enhanced with the restoration of degraded land. Hence, native shrub restoration efforts can be justified as re-establishment mechanisms to provide ecosystem services and conserve habitat for endangered species, as well for the indirect benefits of carbon accumulation in vegetation and soil (Luo et al. 2007).

Global climate models predict that increased temperature and higher evaporative demand are likely to reduce shrubland productivity (Emmett et al. 2004; IPCC 2007; de Dato et al. 2010; Yang et al. 2011) and show the importance of monitoring shrubland ecosystems in the future. The restoration of shrublands is also vital for wildlife conservation to ensure localized recovery of natural ecosystem functions. Our attempts to assess shrubland restoration over a large area provide an opportunity to evaluate the efficacy of habitat restoration efforts at the landscape scale and help to better understand the role of various factors that influence the restoration process such as disturbance regimes, ecological processes, environmental factors, and community structure (Holmes 2001). One of the goals of native shrub restoration is to link fragmented habitats with newly established patches to create areas large enough to maintain viable local populations of targeted species. Since restored patches are key in biodiversity conservation (Bennett 1998), remote sensing techniques such as those presented here can help managers better quantify the pace and scale of restoration success.

Conclusion

We demonstrated that individual shrub A_C derived from remote sensing images could be used to determine shrub

density and estimate biomass across a large area. Although accurate delineation of individual shrub crowns and estimation of A_C are challenging, the method described here provides a basis for application to similar shrublands elsewhere. Estimation of shrub biomass from aerial images showed plant responses to broad environmental gradients and included evaluation of some impacts of past land management. Since management paradigms are often based on inventories of woody plants, automated individual plant delineation as demonstrated here could be an important step in providing rapid and spatially extensive stand information for effective management. This approach has the potential to assess plant density and biomass over a larger extent of landscape. Particularly, plant delineation from remote sensing data helped us to evaluate the restoration of native shrublands.

Considering that 90 % of native vegetation cover in LRGVNWR has been removed since the 1930s, successful reestablishment of the woody shrub plant community in the refuge during the last two decades has resulted in some success. Replantation of native shrubs was shown in this study to be equally as effective as natural regeneration in developing large and productive shrub stands contributing to wildlife habitat conservation and carbon sequestration. The study showed that these woody shrublands are potential carbon sinks and can potentially be used as carbon credits to encourage further land acquisition for conservation and carbon sequestration.

Appendix A

See Table 3.

Table 3 Equations used to predict live biomass (*LB*; g) from canopy area (*CA*; m^{-2}) for six woody species in southern Texas thorn woodland (Northup et al. 2005)

Species	Biomass equation	Correction factor
Vachellia rigidula (VARI)	Ln (LB) = 6.316 + 1.465(LnCA)	1.005
Celtis ehrenbergiana (CEEH)	Ln (LB) = 6.782 + 1.406(LnCA)	1.018
Condalia hookeri (COHO)	Ln (LB) = 7.088 + 1.488(LnCA)	1.004
Diospyros texana (DITE)	Ln (LB) = 7.343 + 1.439(LnCA)	1.009
Prosopis glandulosa (PRGL)	Ln (LB) = 6.873 + 1.482(LnCA)	1.005
Zanthoxylum fagara (ZAFA)	Ln (LB) = 7.049 + 1.213(LnCA)	1.008

References

Adhikari A, White JD (2014) Plant water use characteristics of five dominant shrub species of the Lower Rio Grande Valley, Texas, USA: implications for shrubland restoration and conservation. Conserv Physiol 2. doi:10.1093/conphys/cou005

Adhikari A, White JD (2016) Climate change impacts on regenerating shrubland productivity. Ecol Model 337:211–220. doi:10.1016/j.ecolmodel.2016.07.003

Anaya JA, Chuvieco E, Palacios-Orueta A (2009) Above ground biomass assessment in Colombia: a remote sensing approach. For Ecol Manage 257:1237–1246

Archer S (1989) Have southern Texas savannas been converted to woodlands in recent history? Am Nat 134:545–561

Asner GP, Knapp DE, Balaji A, Paez-Acosta G (2009) Automated mapping of tropical deforestation and forest degradation: CLASlite. J Appl Remote Sens 3:033543. doi:10.1117/1.3223675

Bechtold HA, Inouye RS (2007) Distribution of carbon and nitrogen in sagebrush steppe after six years of nitrogen addition and shrub removal. J Arid Env 71:122–132

Bennett AF (1998) Linkages in the landscape: the role of corridors and connectivity in wildlife conservation. IUCN, Gland

Blair WF (1950) Biotic provinces of Texas. Tex J Sci 2:93–117

Blanco P, Navarro RM (2003) Aboveground phytomass models for major species in shrub ecosystems of western Andalusia. Invest Agrar Sist Recur For 12:47–55

Burquez A, Martinez-Yrizar A, Nunez S, Quintero T, Aparicio T (2010) Aboveground biomass in three Sonoran Desert communities: variability within and among sites using replicated plot harvesting. J Arid Environ 74:1240–1247

Clark DB, Read JM, Clark ML, Cruz AM, Dotti MF, Clark DA (2004) Application of 1-m and 4-m resolution satellite data to ecological studies of tropical rain forests. Ecol Appl 14:61–74

Colwell JE (1974) Vegetation canopy reflectance. Remote Sens Environ 3:175–183

Culvenor DS (2002) TIDA: an algorithm for the delineation of tree crowns in high spatial resolution remotely sensed imagery. Comput Geosci 28:33–44

de Dato GD, Angelis PD, Sirca C, Beir C (2010) Impact of drought and increasing temperatures on soil CO_2 emissions in a Mediterranean shrubland (gariga). Plant Soil 327:153–166

Eddy MR, Judd FW (2003) Phenology of *Acacia berlandieri*, *A. minuata*, *A. rigidula*, *A. schaffneri*, and *Chloroleucon ebano* in the Lower Rio Grande Valley of Texas during a drought. Southwest Nat 48:321–332

Emmett BA, Beier C, Estiarte M, Tietema A, Kristensen HL, Williams D, Penuelas J, Schmidt I, Sowerby A (2004) The response of soil processes to climate change: results from manipulation studies of shrublands across an environmental gradient. Ecosystems 7:625–637

Erickson M, Olofsson K (2005) Comparison of three individual tree crown detection methods. Mach Vis Appl 16:258–265

Gilabert MA, Gonzalez-Piqueras J, Garcia-Haro FJ, Melia J (2002) A generalized soil-adjusted vegetation index. Remote Sens Environ 82:303–310

Gougeon FA (1995) A crown-following approach to the automatic delineation of individual tree crowns in high spatial resolution aerial images. Can J Remote Sens 21:274–284

Helmer EH, Ruefenacht B (2005) Cloud-free satellite image mosaics with regression trees and histogram matching. Photogramm Eng Remote Sens 71:1079–1089

Holdway RJ, Allen RB, Clinton PW, Davis MR, Coomes DA (2008) Intraspecific changes in forest canopy allometries during self-thinning. Funct Ecol 22:460–469

Holmes HM (2001) Shruland restoration following woody alien invasions and mining: effects of topsoil depth, seed source, and fertilizer addition. Rest Ecol 9:71–84

Huete AR (1988) A soil-adjusted vegetation index (SAVI). Remote Sens Env 25:295–309

Hughes HG, Varner LW, Blankenship LH (1987) Estimating shrub production from plant dimensions. J Range Manage 40:367–369

IPCC (2007) Climate change 2007: the physical science basis. Contribution of Working Group I to the fourth assessment report of the Intergovernmental Panel on Climate Change. Cambridge University Press, Cambridge

Jahrsdoerfer SE, Leslie DM (1988) Tamaulipan brushland of the Lower Rio Grande Valley of Texas: description, human impacts, and management options. Biological report 88. US Fish and Wildlife Service, US Department of Interior

Katoh M, Gougeon FA, Leckie DG (2009) Application of high-resolution airborne data using individual tree crowns in Japanese conifer plantations. J For Res 14:10–19

Kettrings QM, Coe R, van Noordwijk M, Ambagau Y, Palm CA (2001) Reducing uncertainty in the use of allometric biomass equations for predicting above-ground tree biomass in mixed secondary forests. For Ecol Manage 146:199–209

Koch B, Heyder U, Weinacker H (2006) Detection of individual tree crowns in airborne Lidar data. Remote Sens Environ 72:357–363

Lal R (2004) Carbon sequestration in dryland ecosystems. Environ Manage 33:528–544

Laliberte AS, Rango A, Havstad KM, Paris JF, Beck RF, McNeely R, Gonzalez AL (2004) Object oriented image analysis for mapping shrub encroachment from 1937–2003 in southern New Mexico. Remote Sens Environ 93:198–210

Lambers H, Capin FS III, Pons TL (1997) Plant physiological ecology. Springer, New York, p 25

Larsen M, Rudemo M (1998) Optimizing templates for finding trees in aerial photographs. Pattern Recogn Lett 19:1153–1162

Li B, Wu H, Zou G (2000) Self-thinning rule: a causal interpretation from ecological field theory. Ecol Model 132:167–173

Lioubimtseva E, Adams J (2004) Possible implications of increased carbon dioxide levels and climate change for desert ecosystems. Environ Manage 33:S388–S404

Litton CM, Kauffman JB (2008) Allometric models for predicting above-ground biomass in two widespread woody plants in Hawaii. Biotropica 40:313–320

Luo H, Oechel WC, Hastings SJ, Zulueta R, Qian Y, Kwon H (2007) Mature semiarid chaparral ecosystems can be a significant sink for atmospheric carbon dioxide. Glob Change Biol 13:386–396

Luyssaert S, Schulze E-D, Bőrner A, Knohl A, Hessenmőller D, Law BE, Ciais P, Grace J (2008) Old-growth forests as global carbon sinks. Nature 455:213–215

Lyon JG, Yuan D, Lunetta RS, Elvidge CD (1998) A change detection experiment using vegetation indices. Photogramm Eng Remote Sens 64:143–150

Major DJ, Baret F, Guyot G (1990) A ratio vegetation index adjusted for soil brightness. Int J Remote Sens 11:727–740

Mitchell HB (2010) Image fusion: theories, techniques, and application. Springer, Berlin

Montagu KD, Woo KC (1999) Recovery of tree photosynthetic capacity from seasonal drought in the wet-dry tropics: the role of phyllode and canopy processes in *Acacia auriculiformis*. Aust J Plant Physiol 26:135–145

Navar J (2011) Plasticity of biomass component allocation patterns in semiarid Tamulipan thornscrub and dry temperate pine species of northeastern Mexico. Polibotanica 31:121–141

Navar J, Mendez E, Dale V (2002) Estimating stand biomass in the Tamaulipan thornscrub of northeastern Mexico. Ann For Sci 59:813–821

Navar J, Mendez E, Najera A, Graciano J, Dale V, Parresol B (2004) Biomass equations for shrub species of Tamaulipan thornscrub of north-eastern Mexico. J Arid Environ 59:657–674

Navar-Chaidez JDJ (2008) Carbon fluxes resulting from land-use change in the Tamaulipan thornscrub of northern Mexico. Carbon Balance Manage 3:6. doi:10.1186/1750-0680-3-6

Northup BK, Zitzer SF, Archer S, McMurtry CR, Boutton TW (2005) Above-ground and carbon and nitrogen content of woody species in a subtropical thornscrub parkland. J Arid Environ 62:23–43

Patterson D (2011) ArcGIS Bounding Containers Sept 28, 2011. http://www.arcgis.com/home/item.html?id=564e2949763943e3b9fb4240bab0ca2f

Peltzer DA, Köchy M (2001) Competitive effects of grasses and woody plants in mixed-grass prairie. J Ecol 89:519–527

Piao S, Fang J, Ciais P, Peylin P, Huang Y, Sitch S, Wang T (2009) The carbon balance of terrestrial ecosystems in China. Nature 458:1009–1013

Pollock R (1994) A model-based approach to automatically locating individual tree crowns in high-resolution images of forest canopies. In: Proceedings of the First International Airborne Remote Sensing Conference and Exhibition, 12–15 September 1994, Strasbourg, pp 11–15

Qi J, Chehbouni A, Huete AR, Kerr YH, Sorooshian S (1994) A modified soil adjusted vegetation index. Remote Sens Environ 48:119–126

Richards JA, Xiuping J (1993) Remote sensing digital image analysis: an introduction, 4th edn. Springer, Berlin

Rodriguez HG, Silva IC, Gomez Meza MV, Lozano RGR (2004) Plant water relations of thornscrub shrub species, north–eastern Mexico. J Arid Environ 58:483–503

Schlossberg S, King DI, Chandler RB, Mazzei BA (2010) Regional synthesis of habitat relationships in shrubland birds. J Wildl Manage 74:1513–1522

Stow D, Hamada Y, Coulter L, Anguelova Z (2008) Monitoring shrubland habitat changes through object-based change identification with airborne multispectral imagery. Remote Sens Environ 112:1051–1061

Suganuma H, Abe Y, Taniguchi M, Tanouchi H, Utsugi H, Kojima T, Yamada K (2006) Stand biomass estimation method by canopy coverage for application to remote sensing in an arid area of Western Australia. For Ecol Manage 222:75–87

Thompson FR, DeGraaf RM (2001) Conservation approaches for woody, early successional communities in the eastern United States. Wildl Soc Bull 29:483–491

Tremblay TA, White WA, Raney JA (2005) Native woodland loss during the mid-1900s in Cameron County, Texas. Southwest Nat 50:479–519

US Fish and Wildlife Service (2013) Gulf coast jaguarundi (*Puma yagouaroundi cacomitli*) recovery plan, first revision. US Fish and Wildlife Service, Albuquerque

US Fish and Wildlife Service (2016) Recovery plan for the ocelot (*Leopardus pardalis*), first revision. US Fish and Wildlife Service, Albuquerque

Van Auken OW (2000) Shrub invasions of North American semiarid grasslands. Annu Rev Ecol Syst 31:197–215

Wang L, Gong P, Biging GS (2004) Individual tree-crown delineation and treetop detection in high-spatial-resolution aerial imagery. Photogramm Eng Remote Sens 70:351–358

Wenhiu L, Jiaojun Z, Quanquan J, Xiao Z, Jhunsheng L, Xuedong L, Lile H (2014) Carbon sequestration effects of shrublands on Three-North Sheltbelt Forest region, China. Chin Geogr Sci 24:444–453

White JD (2001) Size and biomass relationships for five common northern Chihuahuan desert plant species. Tex J Sci 53:385–389

Wulder M, Niemann KO, Goodenough D (2000) Local maximum filtering for the extraction of tree locations and basal area from high spatial resolution imagery. Remote Sens Environ 73:103–114

Yang X, Lo CP (2000) Relative radiometric normalization performance for change detection from multi-date satellite images. Photogramm Eng Remote Sens 8:967–980

Yang H, Wu M, Liu W, Zhang Z, Zhang N, Wan S (2011) Community structure, composition in response to climate change in a temperate steppe. Glob Change Biol 17:452–465

Yao J, Murray DB, Adhikari A, White JD (2012) Fire in a sub-humid woodland: the balance of carbon sequestration and habitat conservation. For Ecol Manage 2080:40–51

Zeidler J, Hanrahan S, Scholes M (2002) Land-use intensity affects range condition in arid to semi-arid Namibia. J Arid Environ 52:389–403